Assessment of masonry buildings subjected to landslide by using the load path method

F. Palmisano[1],* A. Elia[2]

Abstract

The increase in the computational capabilities in the last decade has allowed numerical models to be widely used in the analysis, leading to a higher complexity in structural engineering. This is why simple models are nowadays essential because they provide easy and accessible understanding of fundamental aspects of the structural response. Accordingly, this article aims at showing the utility and effectiveness of a simple method (i.e. the Load Path Method) in the interpretation of the behaviour of masonry buildings subjected to foundation settlements due to landslide. Models useful for understanding brick-mortar interface behaviour as well as the global one are reported. The global proposed approach is also validated by using Bi-directional Evolutionary Structural Optimization method.

Moreover, drawing inspiration from a case study, the article shows that the proposed approach is useful for the diagnosis of crack patterns of masonry structures subjected to landslide movements.

Keywords: Masonry structures, Settlements, Landslide, Strut-and-tie model, Load path method, BESO method.

1. Introduction

The assessment of landslide risk is a research topic of increasing interest all over the world due to both an increasing awareness of the dramatically important impact of landslides on the socio-economic environment and an increasing request for development and extension of urbanisation in areas prone to landsliding ([1]-[7]). In Italy this problem is particularly relevant in the areas located in the southern Apennines, where landsliding is widespread and responsible for frequent damages to structures and infrastructures.

According to Roca et al. [8], the effort invested during past decades on the numerical modelling of masonry structures has yielded versatile and very accurate computer approaches applicable to a wide variety of problems. Most applications are based on finite element modelling, macro or micro-modelling or discontinuous methods. Moreover a large effort is now being undertaken in the development of homogenization techniques [9]. The availability of these powerful tools has opened new possibilities to the development of more simplified and engineering oriented methods thanks to the larger opportunities given for a comprehensive and reasonably economical validation and calibration.

In this scenario, simple methods based on fundamental

* Corresponding author: f.palmisano@poliba.it
1 DICATECh, Politecnico Bari, Via E. Orabona 4, Bari, Italy
2 PPV Consulting, Via G. Matteotti 37, Bari, Italy

principles, such as the limit theorems of plasticity, are valuable because they provide easy and accessible understanding on fundamental aspects of the structural response. For that purpose, they need to show reasonable simplicity while affording the description of the essential phenomena governing the structural capacity [8]. Among this category, the Strut-and-Tie Model (STM hereafter [10]) has been successfully used for a long time to study reinforced and pre-stressed structures [11].

The possibility of using the STM approach for the study of masonry structural behaviour has been recently investigated (e.g. [8], [12], [13]).

However, despite of all its unquestionable advantages, the strut-and-tie method is not widely disseminated because of several constraints to its practical application. One of the aspects frequently pointed out is the uncertainty in selecting a suitable model leading to the discussion on the validity and uniqueness of models. Moreover, some engineering judgment is required to come up with the design model and to find an equilibrated strut-and-tie model can be time consuming if the designer is not familiarized with the technique [14]. This is the reason why in this article the Load Path Method is proposed as an instrument to design strut-and-tie models in masonry structures.

Following what above mentioned, this article aims at showing the effectiveness of a simple method (i.e. the Load Path Method) in the interpretation of the behaviour of masonry buildings subjected to foundation settlements due to landslide.

In fact, one of the main difficulties, when dealing with

landslide structural vulnerability, is the possibility to individuate the causes of a crack pattern. Models based on classical structural mechanics are often difficult to apply especially when there is the necessity to perform a rapid vulnerability assessment at the territorial scale. These are the cases in which the Load Path Method shows its utility and effectiveness.

Moreover, the choice of the Load Path Method as an instrument to investigate structural behaviour derives from the wish to find a method that could represent the 'trait d'union' between Structure and Architecture.

The absence of a common language is one of the reasons why nowadays there is a very big gap between the architect and the engineer.

Architects are always involved in restoration work and, hence, in the evaluation of structural vulnerability.

Nowadays, when dealing with landslide vulnerability assessment, there is a huge need to bridge the gap between architects and engineers. Maybe it can be achieved by finding a common model that should be a method to understand structural behaviour as well as a clear and effective instrument of investigation and judgement. A method not only numerical but also geometrical that should predict calculation results disclosing the shape aspects from which it is possible to recognise the real structural behaviour.

In this context, this article aims to highlight that the Load Path Method seems to open new perspectives in the search for a common language between engineers and architects to try to give voice, in harmony and in a single design, to formal, aesthetical, functional and structural aspects.

Differently from what proposed by [8] and [13], the proposed approach is not aimed at quantifying the ultimate capacity of masonry walls in the above mentioned conditions, but it intends to show the effectiveness of the Load Path Method for the prediction of structural behaviour as well as for the diagnosis of the crack patterns. Moreover, it is worth noting that while the approach of [8] and [13] is based only on equilibrium models, the proposed approach is based also on consistency.

2. Key Features Of The Load Path Method

Born as a method to design strut-and-tie models in reinforced concrete structures, the Load Path Method (LPM hereafter) was introduced by Schlaich et al. [11] and then developed mainly by F. Palmisano and A. Vitone (e.g. references [15]-[19]). Vitone, C. [20], De Tommasi et al. [21], Palmisano et. al. [22], Palmisano & Totaro [23], Palmisano [24], [25] proposed the Load Path Method to analyse also the behaviour of masonry structures.

In the transfer of forces within a structure or an element, from their point of origin (S) to their ends (E), deviations in the load path direction can occur causing a thrust (H); for equilibrium to be maintained, a reactive force must be applied that is equal in magnitude and opposite in direction to this thrust (Figs. 1 and 2).
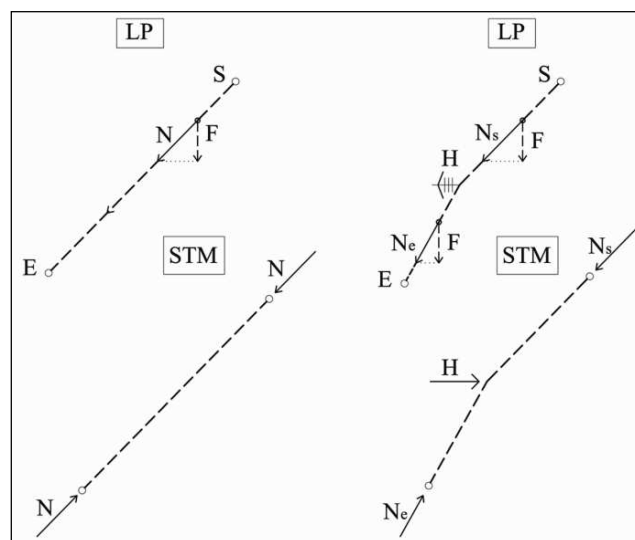

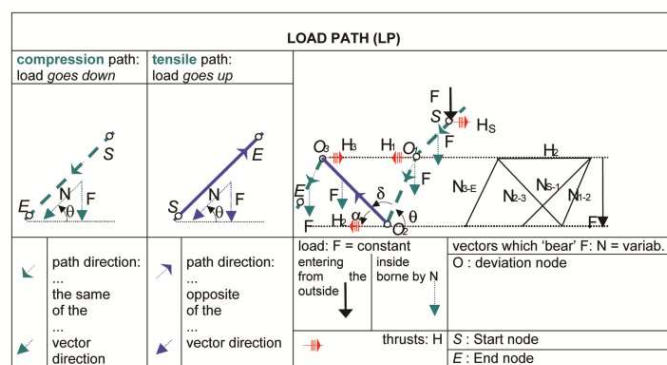**Fig. 1.** Load Path (LP) and Strut-and-Tie Model (STM)

Fig. 2. Load Path: symbols

The load path represents the line along which a force or a force component (more precisely: the component of a force in a chosen direction, e.g. the vertical component of a load) is carried through a structure from the point of loading to its support. The force component (F in Fig. 1) associated with a load path remains constant on its way through the structure; as a consequence of this definition, thrust H must be perpendicular to the travelling load F. The design of this load flowing through the structure can be approximated by polygonal lines in which there are thrusts in every deviation node.

It follows that, according to the model, the structure will be crossed by fluxes in compression (dashed lines), when loads travel in the same direction of their path, and by fluxes in tension (continuous lines) along which loads go in the opposite direction with respect to their path (Fig. 2). According to the classical theory, the basic principles of the Load Path Method are the respect of both equilibrium and consistency. Thrusts in deviation nodes are necessary in order to respect equilibrium and every path is possible if it is in equilibrium.

Among infinite paths in equilibrium, loads have to choose the one in which their vectors invest the minimum quantity of strain energy (D), that is the only one both consistent and in equilibrium.

The total invested strain energy is

$$D = \frac{1}{2} \int_V \boldsymbol{\sigma} \boldsymbol{\varepsilon} dV \qquad (1)$$

where V is the integration domain, σ and ε are the stress and the strain vector respectively.

Along a generic path, that is polygonal in this model, the calculus of the invested strain energy (D) is simplified in the summation of the terms which are relative to each side of the truss:

$$D = \sum_i D_i \qquad (2)$$

where i is the generic side of the load path.

For instance, if linear elastic constitute laws for materials are assumed as well as constant transversal section of each side, the elementary strain energy D_i is

$$D_i = \frac{1}{2} N_i l_i \varepsilon_i \qquad (3)$$

where i is the generic side of the load path, N_i is the intensity of the vector that bears the travelling load on that side, l_i is the length of the generic side and ε_i is the mean strain on that side.

In the assumption of linear elastic constitute laws for materials with Young's Modulus equal to E, if the transversal section of a side is linearly variable from $A^{(1)}_i$ to $A^{(2)}_i$ (e.g. half of a bottle-shaped strut) the elementary strain energy D_i is

$$D_i = \frac{1}{2} \frac{N_i^2 l_i}{E\left(A_i^{(1)} - A_i^{(2)}\right)} Ln\left(\frac{A_i^{(1)}}{A_i^{(2)}}\right) \qquad (4)$$

From figure 2 it is possible to notice that the relation between the travelling load F and its vector N is

$$N = \frac{F}{\sin\theta} \qquad (5)$$

where θ is the inclination of the path. If θ decreases, N increases; this means that the condition with θ nil is not consistent because it will produce an infinite value of N and, hence, of the strain energy D. The consequence of this consideration is that a travelling load cannot move orthogonally to itself. The only possibility to move in the direction orthogonal to the travelling load is to follow a path composed by inclined descending and ascending sides.

3. Behaviour at the Brick-Mortar Interface

In the next paragraph it will be shown that in a masonry wall subjected to foundation settlements due to landslide, load paths in tension arise. This is the reason why in this paragraph micro-models principally referred to the brick-mortar interface when crossed by tension fluxes are presented [26].

As told at the end of paragraph 1, the proposed

approach is not aimed at quantifying the ultimate capacity of masonry walls when subjected to landslide movements but it is aimed at showing the effectiveness of the Load Path Method for the prediction of structural behaviour as well as for the diagnosis of the crack patterns. In this scenario the aim of this paragraph is simply to re-interpret, by using the Load Path Method, the mechanisms that permit tension fluxes to cross a brick-mortar interface in a masonry wall.

In this paragraph and in the following one, for the sake of shortness, only the main and peculiar aspects of the figures are described. For further details see references [15]-[19].

Figure 3 shows the adopted geometrical model; the morphology of the brick sides is characterised by 'dents' and 'hollows'.

The following assumptions have been made:
- masses are concentrated;
- the brick-mortar joint can be crossed only by a path in compression;
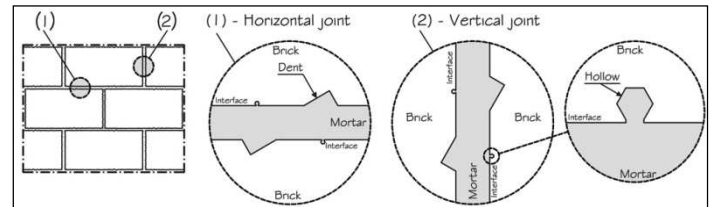- only load paths perpendicular to the contact surface can cross the interface.

Fig. 3. Geometrical model of the brick-mortar interface.

The micro-models proposed in this paragraph show the path followed by the travelling load F and by its elementary parts F_i in a masonry wall subjected to a tension flux. 'Friction' and 'adhesion' are the main mechanisms that can be activated to make the tension fluxes cross the brick-mortar interface. These mechanisms are strictly connected to the characteristics of the two materials. Friction and adhesion can be physically modelled respectively by 'micro-dents' and 'micro-hollows' on the side of the brick.

In Figure 4 the model for the friction mechanism from the scale of the whole masonry wall (i.e. at the global scale) to a smaller scale (i.e. at the local scale, see details (1), (2), (3) in Fig. 4) is represented.

The detail (1) of figure 4 shows a possible path of the weight of the brick where the elementary component F_i divides itself into two equal parts because of the symmetry condition. It is worth noting that this symmetry condition should be both geometrical and mechanical. For instance, if the tension Young's modulus is less than the compression one, the compression 'descending' path in the detail (1) of figure 4 is followed by a larger part of F_i.

The details (2) and (3) of figure 4 show the paths of loads and thrusts at the brick-mortar interface. Thanks to the brick dents, load passes from brick to mortar, crossing the interface using a compression path. In every deviation node, the elementary travelling load applies an additional thrust that has to find equilibrium in the structure.

A peculiarity of the friction mechanism is that this can

F. Palmisano, A. Elia

be activated also without mortar at the interface; it is only necessary the contact between the two surfaces. In this case two negative effects arise. Firstly, the reduction in the crossing surface dimension causes a stress increase in the contact area. Secondly, the deviation of the elementary parts F_i towards the contact area causes new additional thrusts and then new stresses in the brick.
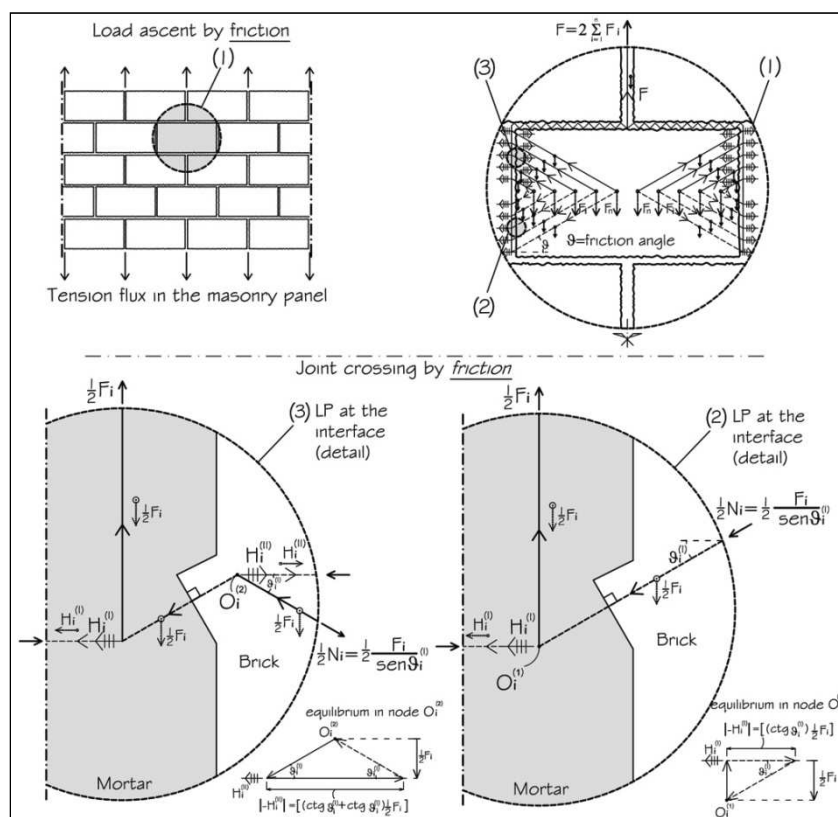

Fig. 4. Friction mechanism

Figures 5 and 6 show models for the adhesion mechanism that is defined as the penetration of a material into a different one. To activate this mechanism it is necessary that at least one of the two materials, in the penetration phase, has different granulometry and consistency. Bricks and mortar fulfil these requirements thanks to the porosity of the first one and the fluidity of the second one during casting. Figures 5 and 6 show the cases of vertical and inclined ascent.
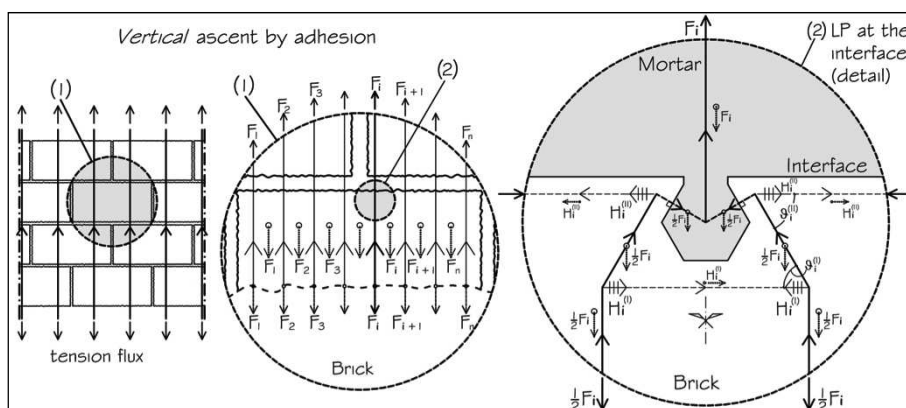

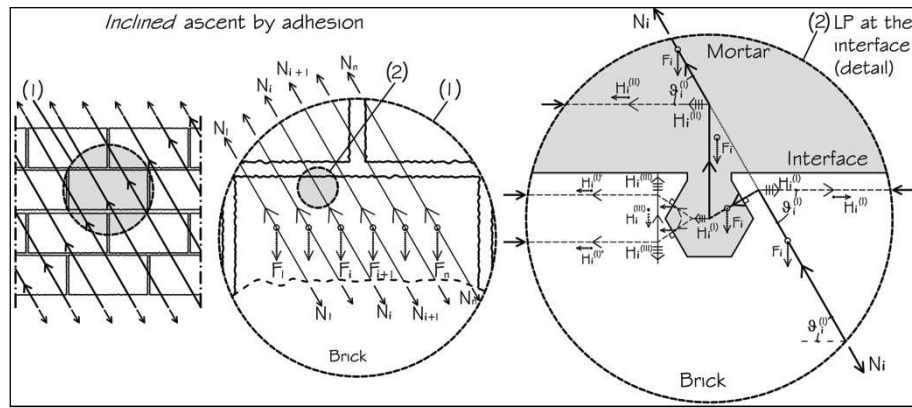**Fig. 5.** Adhesion mechanism: vertical ascent

Fig. 6. Adhesion mechanism: inclined ascent

Regarding the model in figure 5, it is worth noting that while the thrusts $H_i^{(I)}$ can find equilibrium by a direct path in compression, the thrusts $H_i^{(II)}$ (applied in the top deviation nodes) have to find equilibrium in the structure because they cannot cross the hollow by a path in tension.

In the model of the inclined ascent (Fig. 6) F_i has to deviate to enter the hollow by a path in compression; further deviations are necessary in the mortar to make F_i return to the original path. It is worth noting that differently from the vertical ascent model, in this case the travelling load applies thrusts in the mortar, i.e. in the 'weakest' element of the masonry wall.

The two adhesion models clearly show the local stress increase at the brick-mortar interface caused by the deviation of the load paths, by the concentration of the paths and by the generation of further thrusts.

After the definition of the elementary mechanisms, in figures 7 and 8 some models of the mortar-brick joint crossing are proposed. These models show that, because of the generally unlikelihood to have two facing dents or hollows, the travelling load has to undergo deviations inside the mortar joint (in order to pass from brick to mortar and vice versa by using a compression path), stressing the mortar itself by tension paths.
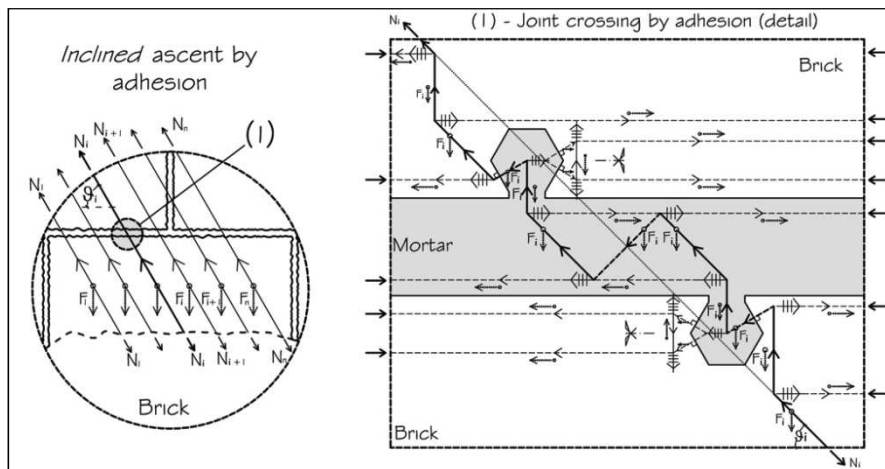

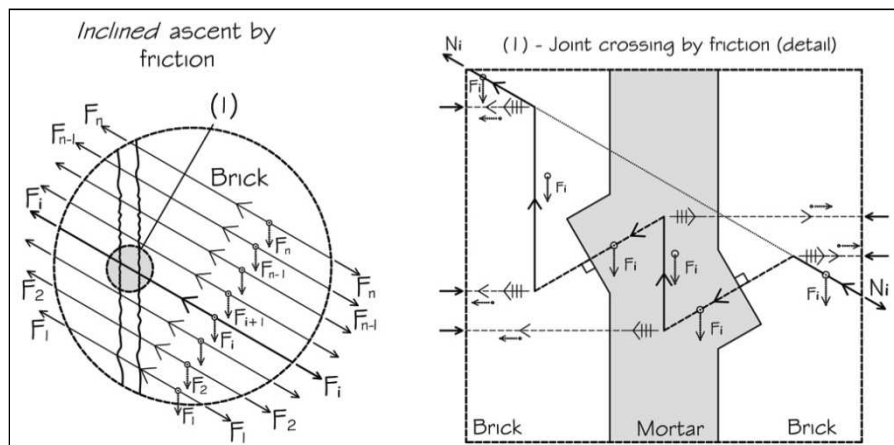**Fig. 7.** Inclined crossing of the horizontal joint by adhesion mechanism

Fig. 8. Inclined crossing of the vertical joint by friction mechanism

316

F. Palmisano, A. Elia

The model effectively highlights both the role of connection performed by the mortar and the necessity of this material to have a sufficient tensile strength. The use of low strength mortar causes a huge decrease of the resistance of the whole masonry wall to the mentioned ascent paths. It follows that particular attention has to be paid to this aspects because these fluxes are due to foundation settlements as well as to seismic actions.

4. Behaviour of a Masonry Panel Subjected to Foundation Settlements

Some macro-models performed by the Load Path Method which show the interpretation of the structural behaviour of a masonry wall subjected to foundation settlements due to landslide are presented in this paragraph.

The following assumptions have to be made:

- settlement is only due to the landslide movement; it does not depend on the loads acting on the masonry wall;
- masses are concentrated;
- the masonry wall is infinitely stiff respect to the foundation soil;
- a perfectly plastic constitutive law at the ultimate limit state has been hypothesised for the soil.

Despite these assumptions, that benefit the simplicity of the analysis, the method has general validity.

Figure 9 [26] shows the structure at the *state 1* (static equilibrium before the soil settlement). In this state, because of the simplicity of the model, there are only descending loads and, in this macro-model, there are no deviations of the travelling loads. Actually, a microscopic analysis would show that travelling loads have to deviate in order to cross the brick-mortar interface [20].
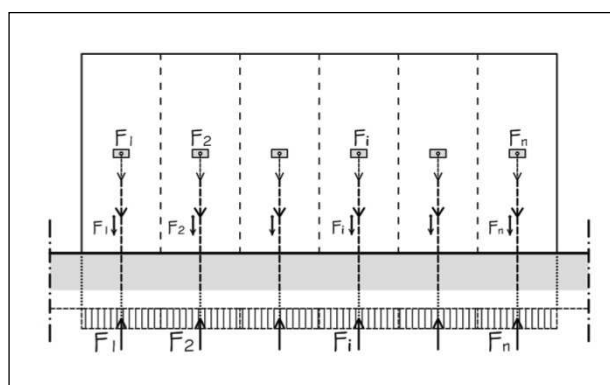

Fig. 9. State 1: static equilibrium condition before the soil settlement

In figures 10-13 ([20], [26]), four different and possible (i.e. in equilibrium) load paths at the *state 2* (after soil settlement), for the case of a settlement that involves the lateral part of a masonry wall ('lateral settlement' hereafter), are represented (i.e. the so-called 'hogging' condition); moreover in figures 10 and 11, the complete strut-and-tie models, obtained from the above mentioned load paths, are shown. The settlement has been modelled as a complete loss of contact between the soil and the right

bottom side of the masonry wall.

Such loss of contact at the soil-wall interface causes the interruption of some load paths of the *state 1*, the relevant modification of the interrupted paths and the modification of other paths in order to restore global equilibrium. It is worth noting that, differently from what shown in figures 10-13, the components F_i should divide themselves into parts which should follow different paths in order to minimise the total strain energy of the system.

Nonetheless, a simplified sketch, representing the whole load which follows a chosen morphology of path, has been reported in the figures. Such assumption seems in fact to be very useful for immediately catching the 'dominant path' (i.e. the one followed by a large part of the total load) in order to enlighten the failure mechanism and the relevant crack pattern.

The models in figures 10-13 make easily catch the effects of the soil settlement on the structure:

- because of equilibrium conditions, soil pressure diagram in *state 2* is different from that of *state 1*; moreover, because of the adopted assumptions, soil pressure is nil on an area symmetrical to the one that has undergone the settlement;
- paths in tension arise in the masonry wall;
- load deviations generate thrusts that can find equilibrium by paths in tension and in compression.

From the visual analysis of the paths in figures 10-13, it can be deduced that combining the *LP(1)* with *LP(3)* there should be a saving in the strain energy, with respect to the shown paths, due to the absence of a thrust path in the middle of the panel. Hence it is possible to introduce a new load path (*LP(5)*; Fig. 14; [26]) in which half of the load follows *LP(1)* and the other half follows *LP(3)*.

In a similar way, in figures 15-19 four different and possible (i.e. in equilibrium) load paths at the *state 2* (after soil settlement), for the case of a settlement that involves the central part of a masonry wall ('central settlement' hereafter), are represented (i.e. the so-called 'sagging' condition).

In figures 10-19 possible (i.e. in equilibrium) load paths for the cases of both lateral and central settlement are shown. As above discussed, only one path respects the equilibrium conditions and, at the same time, minimises the total strain energy of the structural system. For complicated systems, the solution (i.e. the identification of this path) can be found either by FEM analysis or by optimisation algorithms (e.g. [27], [28]). There are many cases in which the search of the 'most plausible solution' instead of the exact solution could be very useful (e.g. for the diagnosis of a crack pattern). The 'most plausible solution' is the path to which, among different equilibrated load paths, is associated the lowest value of the total strain energy. This approach can be carried out by very simple mathematical methods and, in many cases, seems to be very useful because it is able to immediately catch the 'dominant path' (i.e. the one followed by the majority of the total load) in order to highlight, immediately and easily, the failure mechanism and the relevant crack pattern.
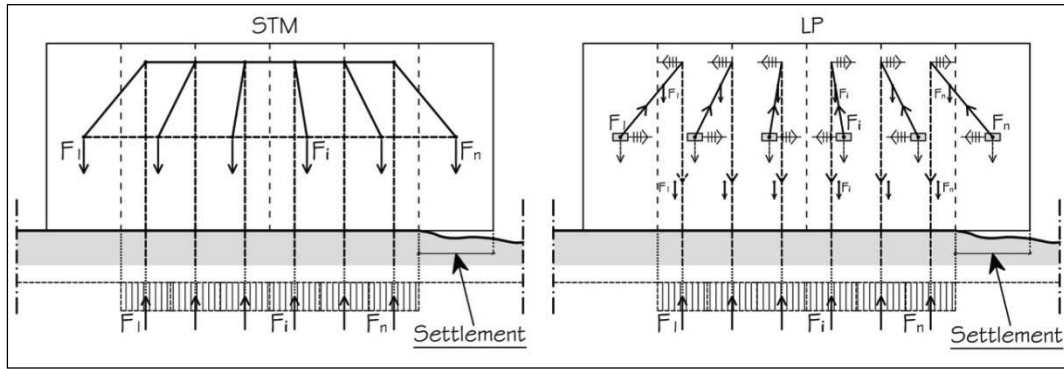
Fig. 10. Settlement that involves the lateral part of a masonry wall. State 2: Load Path LP(1)
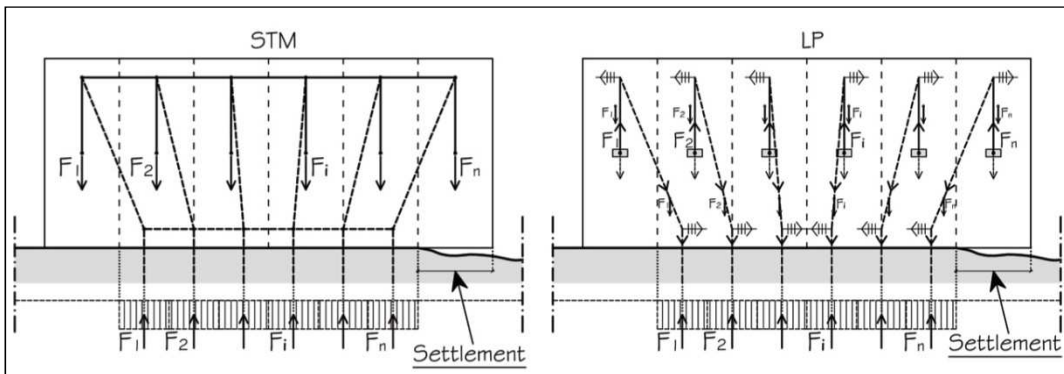

Fig. 11. Settlement that involves the lateral part of a masonry wall. State 2: Load Path LP(2)
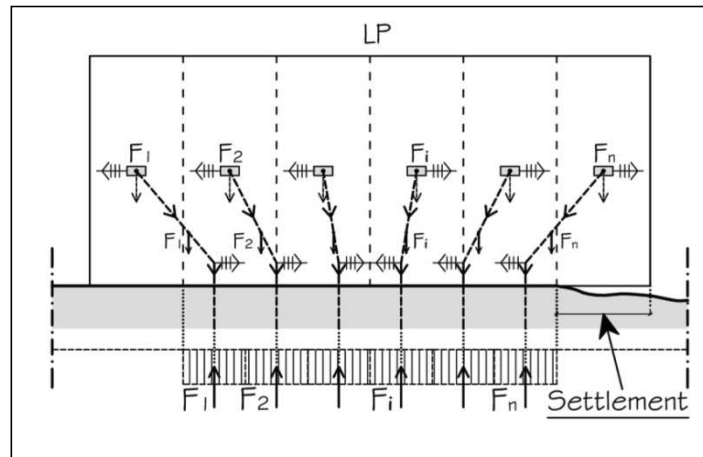

Fig. 12. Settlement that involves the lateral part of a masonry wall. State 2: Load Path LP(3)
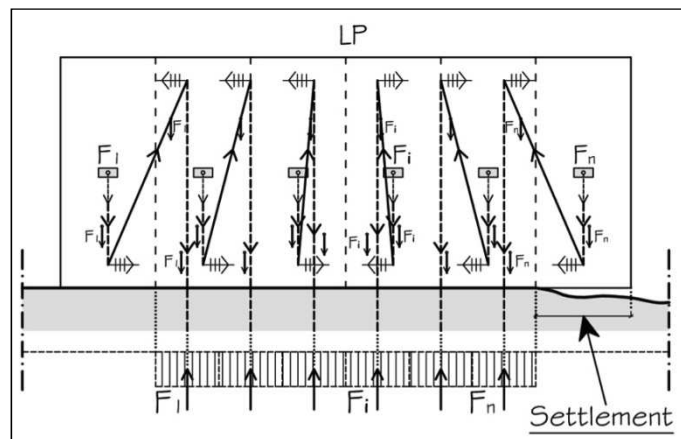

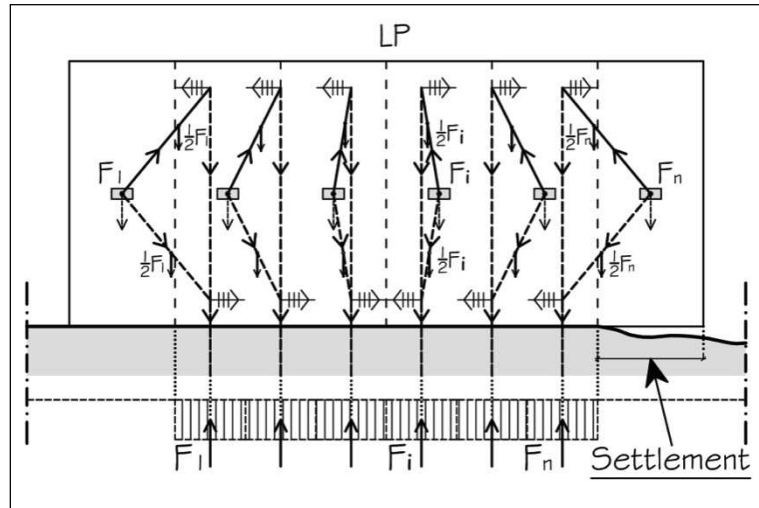**Fig. 13.** Settlement that involves the lateral part of a masonry wall. State 2: Load Path LP(4)

F. Palmisano, A. Elia

Fig. 14. Settlement that involves the lateral part of a masonry wall. State 2: Load Path LP(5); combination of LP(1) with LP(3)
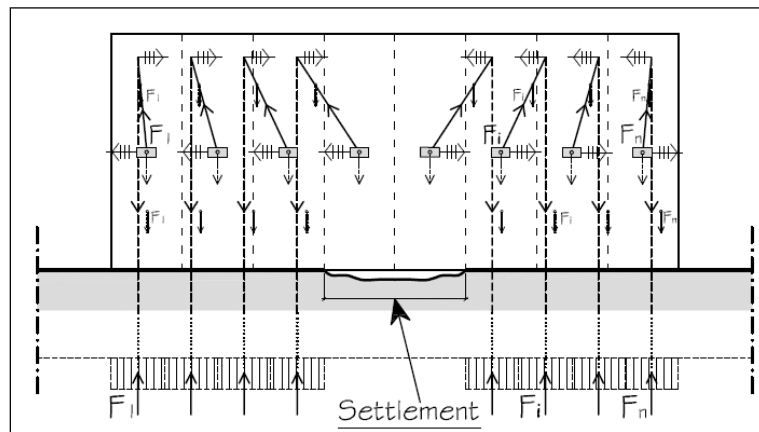

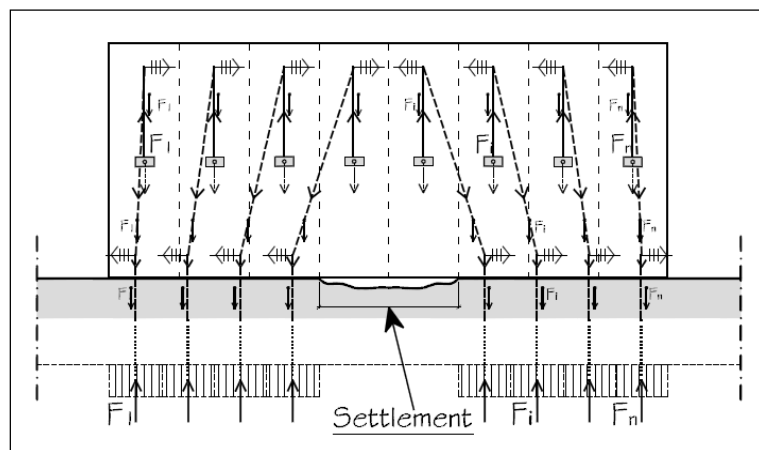**Fig. 15.** Settlement that involves the central part of a masonry wall. State 2: Load Path LP(1)

Fig. 16. Settlement that involves the central part of a masonry wall. State 2: Load Path LP(2)
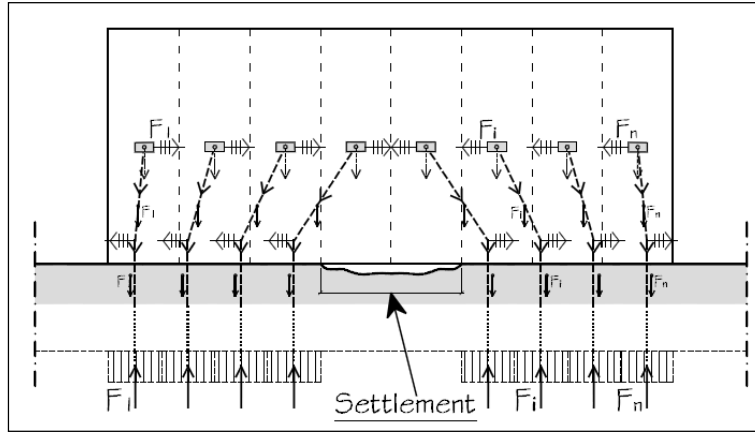
Fig. 17. Settlement that involves the central part of a masonry wall. State 2: Load Path LP(3)
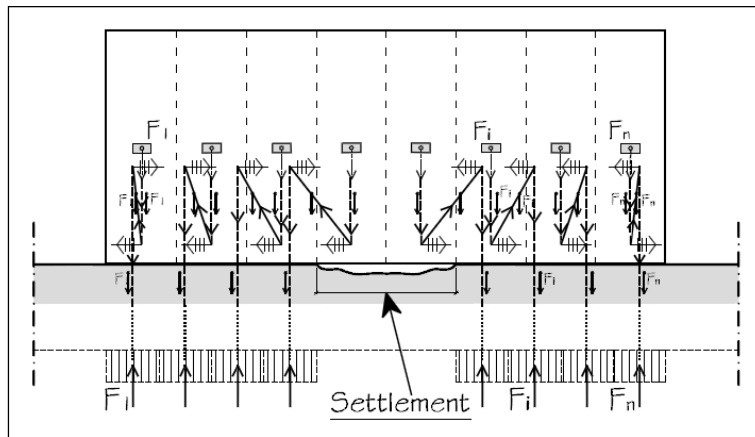

Fig. 18. Settlement that involves the central part of a masonry wall. State 2: Load Path LP(4)
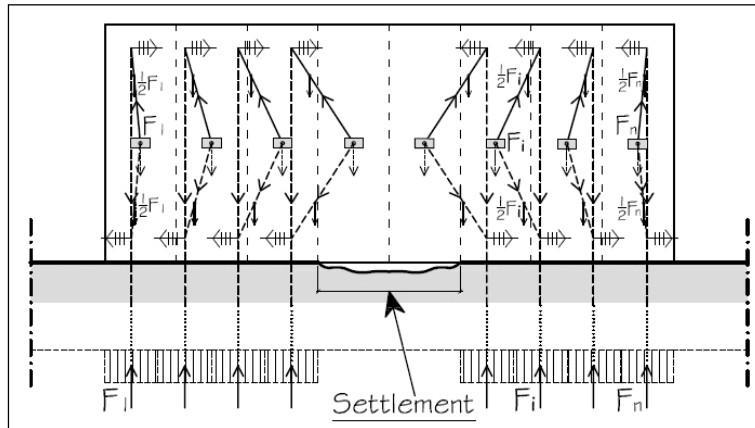

Fig. 19. Settlement that involves the central part of a masonry wall. State 2: Load Path LP(5)

In the following, according to this simplified approach, the energetic analysis of the paths drawn in figures 10-14 is discussed. The masonry wall is considered in *state 2* (i.e. after the soil settlement but before cracking).

In an orthogonal Cartesian system $X\Omega Y$ (where X is the horizontal axis, Y is the vertical axis and Ω is the origin in the middle of the base of the masonry wall; Figs. 20 and 21) the following assumptions have been made:

- the masonry wall is geometrically symmetrical and symmetrically loaded;

- masonry is treated as a homogeneous material;

- the masonry wall is loaded by a uniform gravitational volume load.

Due to symmetry conditions, the analysis can be referred only to half panel. It is worth noting that, thanks to the above-listed assumptions, the load path is symmetrical even though the settlement involves only one side of the panel.
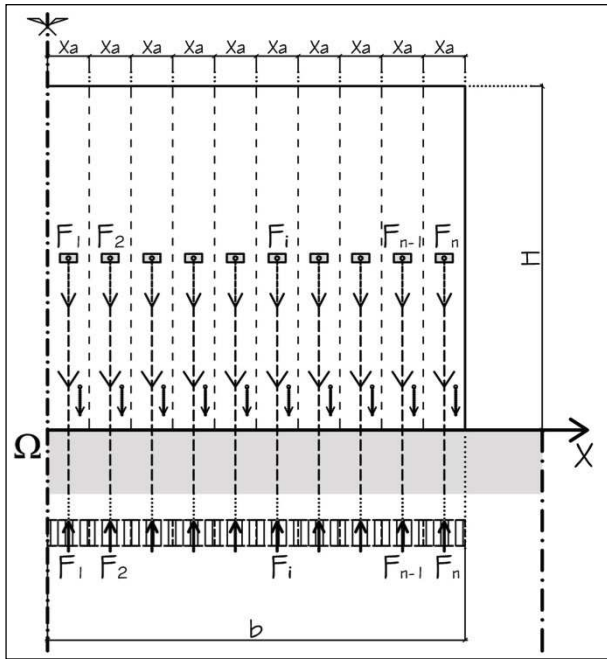
F. Palmisano, A. Elia

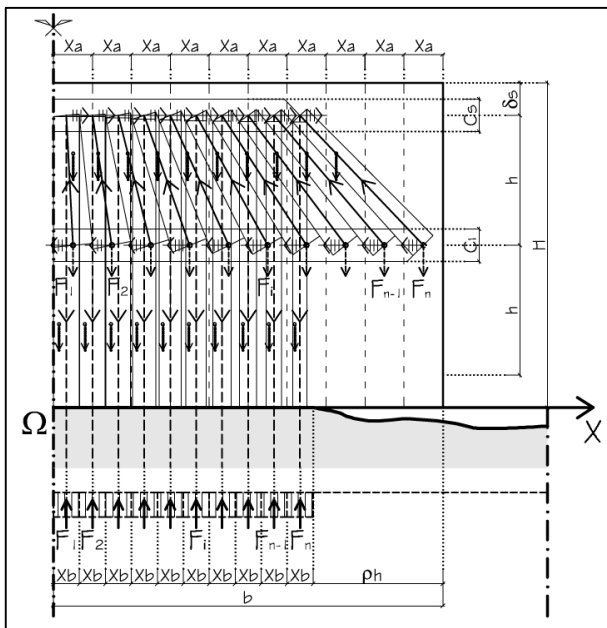**Fig. 20.** State 1: parameters to calculate total strain energy

Fig. 21. Settlement that involves the lateral part of a masonry wall. State 2: parameters to calculate total strain energy of LP(1)

The following parameters have been considered for the masonry wall:

- H is the total height of the wall;
- $B=2b$ is the length of the wall;
- S is the thickness (constant) of the wall;
- $\alpha=\rho \cdot H$ is the length of the soil settlement;
- γ is the unit weight of the wall (i.e. the only load applied at the wall);
- $\omega = E_c/E_s$ is the ratio of the compression Young's Modulus of the wall to the tension one;
- x_a and x_b are the mesh width in the X direction of the panel and of the reactive soil respectively;
- n is the mesh number of the semi-length b of the

panel.

In the following, as an example, the calculus of the strain energy of *LP(1)* is shown; an analogous procedure can be used to calculate strain energy in the other cases.

The following parameters have been used in the analysis (Fig. 21):

- $A_{sup,i}$ and $A_{inf,i}$ are the top and the bottom transversal area of the ith strut;
- θ_i is the inclination of the ith inclined strut;
- A_i is the transversal area of the ith vertical strut;
- δ_s defines the position, along the Y direction, of the load deviation nodes at the top of the wall;
- $h=H/2-\delta_s$;
- C_s and C_i are the width (assumed constant) of the top and of the bottom longitudinal chord.

Strain energy has been calculated by using equations 2, 3 and 4.

The strain energy of the inclined ascent and of the vertical descent is equal to

$$D_{LP1}^{(I)} = \frac{\omega}{2E_c} \sum_{i=1}^{n} \left[\frac{N_i^2 l_i}{(A_{sup,i} - A_{inf,i})} Ln\left(\frac{A_{sup,i}}{A_{inf,i}} \right) \right] \qquad (6)$$

$$D_{LP1}^{(II)} = \frac{H - \delta_s}{2E_c} \sum_{i=1}^{n} \frac{(F_i)^2}{A_i} \qquad (7)$$

respectively, where

$$N_i = \frac{F_i}{sin\theta_i} \qquad (8)$$

$$l_i = \frac{h}{sin\theta_i} \qquad (9)$$

$$\theta_i = \tan^{-1}\left[\frac{2h \cdot n}{\rho H(2i-1)} \right] \qquad (10)$$

The strain energy of the top and bottom longitudinal chord is equal to

$$D_{LP1}^{(sup)} = \frac{1}{2} \frac{\omega \cdot x_b}{E_c \cdot S \cdot C_S} \sum_{j=1}^{n} \left(\sum_{i=1}^{j} \frac{F_i}{\tan\theta_i} \right)^2 \qquad (11)$$

$$D_{LP1}^{(inf)} = \frac{1}{2} \frac{x_a}{E_c \cdot S \cdot C_I} \sum_{j=1}^{n} \left(\sum_{i=1}^{j} \frac{F_i}{\tan\theta_i} \right)^2 \qquad (12)$$

respectively, where

$$\theta_i = \tan^{-1}\left[\frac{2h \cdot n}{\rho H(2i-1)} \right] \qquad (13)$$

Finally the total strain energy of *LP(1)* is

$$D_{TOT}^{LP1} = D_{LP1}^{(I)} + D_{LP1}^{(II)} + D_{LP1}^{(sup)} + D_{LP1}^{(inf)} \qquad (14)$$

To compare the results it is useful to introduce a 'reference strain energy' D_{REF} that is the strain energy invested by the total load of half wall to reach the foundation soil by a vertical direct path in compression (i.e. that invested at *state 1* in Fig. 20). In the examined case the reference strain energy is

$$D_{REF} = \frac{Sb\gamma^2 H^3}{4E_c} \tag{15}$$

In figures 22 and 23 the ratio D_{TOT}/D_{REF} has been plotted for ω equal to 1 and 3 respectively. To plot these diagrams, the following assumptions have been made:

- $H = 6\ m$;

- $B = 18\ m \Rightarrow b = 9\ m$;
- $n = 10$;
- for *LP(1), LP(2)* and *LP(4)* the axis of the top chord is $H/10$ distant from the top edge of the panel;
- for *LP(2), LP(3)* and *LP(4)* the axis of the bottom chord is $H/10$ distant from the bottom edge of the panel;
- the width of the longitudinal chords has been assumed as the maximum value consistent with their positions without causing superimposition of the chords.

The normalised ratio D_{TOT}/D_{REF} quantifies the increase of strain energy in the panel due to settlement and gives the opportunity to immediately catch which is the 'most plausible path' (i.e. the one with the minimum value of the total strain energy).
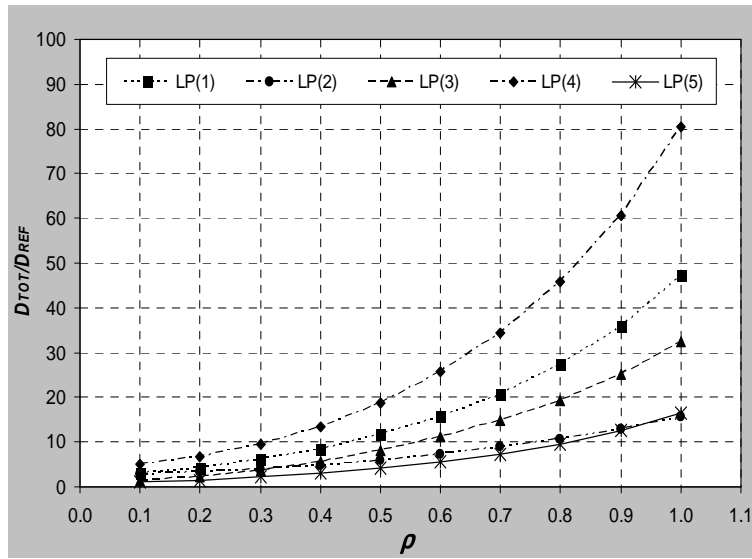

Fig. 22. Settlement that involves the lateral part of a masonry wall. D_{TOT}/D_{REF} in the case of $\omega = 1$

Fig. 23. Settlement that involves the lateral part of a masonry wall. D_{TOT}/D_{REF} in the case of $\omega = 3$

It is worth noting that in all the cases showed in figures 22 and 23, *LP(5)* is the 'most plausible solution'. This is a direct consequence of the above-mentioned consideration about the saving in the strain energy of this load path due

to the elimination of the thrust path in the middle of the panel.

The same approach can be used for the case of central settlement. In figures 24 and 25 the normalised ratio

F. Palmisano, A. Elia

D_{TOT}/D_{REF} has been plotted for ω equal to 1 and 3 respectively. This ratio has been evaluated for the paths drawn in figures 15-19 with the same assumptions of the lateral settlement.

LP(5) is the 'most plausible solution' for ρ lower than

1.2 whereas, for ρ higher than 1.2, the 'most plausible solution' is *LP(2)*. It is worth noting that for $\omega = 1$, if ρ is very low (~0.2), the normalised strain energy ratio of *LP(3)* is almost equal to that of *LP(5)*.

Fig. 24. Settlement that involves the central part of a masonry wall. D_{TOT}/D_{REF} in the case of $\omega = 1$

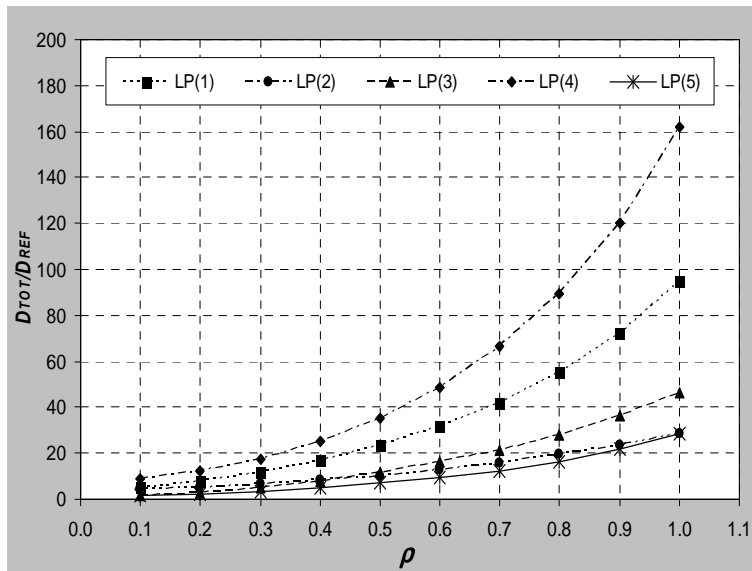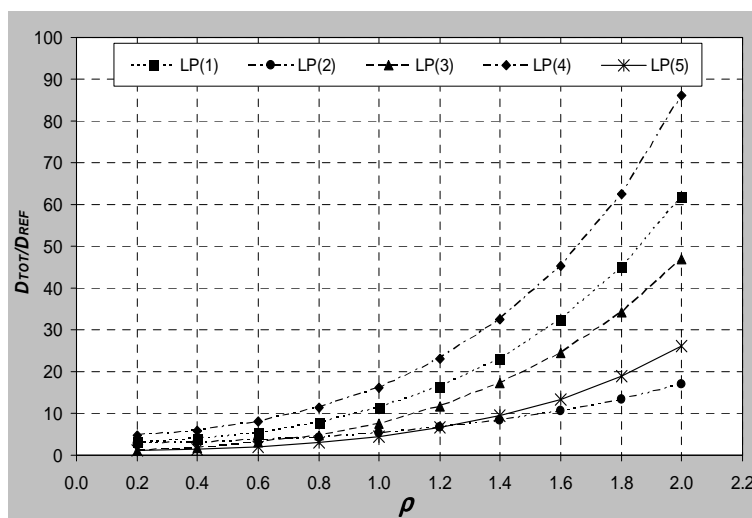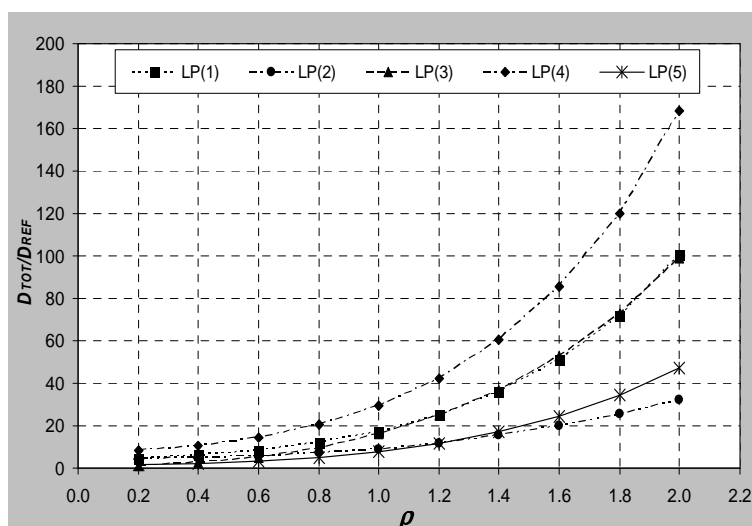**Fig. 25.** Settlement that involves the central part of a masonry wall. D_{TOT}/D_{REF} in the case of $\omega = 3$

As told at the end of paragraph 1, the proposed approach is not aimed at quantifying the ultimate capacity of masonry walls when subjected to landslide movements but it is aimed at showing the effectiveness of the Load Path Method for the prediction of structural behaviour. In this scenario simplified assumptions (e.g. calculus of strain energy in the elastic conditions) seem to be extremely effective.

5. Validation of the Results by Using the Beso Method

In this paragraph the results obtained by the LPM are validated by using an evolutionary optimization procedure.

Shape optimization is a method that enables designers to find a suitable structural layout for the required

performances. The 'Evolutionary Structural Optimization' (ESO) method was first proposed by Xie and Steven [29] in the early 1990s and it has been used to solve a variety of size and shape optimization problems. The basic concept of such a method is that by slowly removing inefficient materials, the structure evolves towards an optimum. The validity of the ESO method depends, to a large extent, on the assumptions that the structural modification (evolution) at each step is small and the mesh for the finite element analysis is dense. If too much material is removed in one step, the ESO method is unable to restore the elements which might have been prematurely deleted at earlier iterations. In order to make the ESO method more robust, a Bi-directional ESO method (BESO) was proposed by Yang et al. [30]. It allows for efficient materials to be added to the structure at the same time as

the inefficient ones are being removed. For further details concerning the BESO algorithm used in the analyses presented in this article see [31].

In order to assist the selection of optimal shapes for the minimum-weight design of continuum structures with stiffness constraints, the performance of the resulting shape at each iteration can be evaluated by a Performance Index PI defined as:

$$PI = \frac{C_0 W_0}{C_i W_i} \qquad (16)$$

where W_0 is the actual weight of the initial domain, C_0 is the strain energy of the initial design under the applied loads, while W_i and C_i are the same quantities of the current design at the *i-th* iteration. It follows that to the optimal configuration will correspond the highest PI.

5.1. Application of the BESO method to a wall subjected to lateral and central settlement

In the following, the application of the BESO method (according to paragraph 5) to the cases shown in paragraph 4 is presented. As previously said the aim is to use the BESO method to validate the results obtained by using the Load Path Method.

The wall has the same dimensions of that described in paragraph 4. The thickness of the wall is 0.30 m.

The numerical analyses have been performed using the Finite Element code ABAQUS 6.7-EF1 [32]. The domain has been subdivided into a regular mesh (0.1 m × 0.1 m) using the linear quadrilateral (type CPS4) finite element. The applied load is only the unit weight of the wall $\gamma = 12$ kN/m^3. Only regarding the applied load, the wall has been divided into ten vertical strips. The uniform applied load has been transformed in ten point loads applied in the centroids of the vertical strips.

The compression Young's modulus of the wall (E_c) and the Poisson's ratio have been assumed equal to 4500 MPa and 0.25 respectively.

The assumed values of γ and E_c are consistent with Table C8A.2.1 of [33] for brick walls whereas the value of the Poisson's ratio is consistent with [34].

Only the cases with $\omega = 1$ have been analysed.

The bottom part of the wall, in the zone not subjected to settlement, is restrained by elastic vertical springs in order to simulate a Winkler soil. The stiffness of the springs is equal to 10 kN/m in order to have a constant soil pressure distribution (as in paragraph 4).

The central node of the bottom of the wall is horizontally fixed. It has been checked that there are no analyses in which this node is removed.

The BESO3D software adopted for the analyses is developed and provided by 'Innovative Structures Group', RMIT University, Australia (www.isg.rmit.edu.au).

The BESO parameters are $ER = 0.5\%$, $AR_{max} = 1\%$, $r_{min} = 0.3$ m (three times the size of one element) and $\tau = 0.1\%$.

Both the cases of lateral and central settlement have been analysed. For the first case analyses for $\rho = 0.3$, $\rho =$

0.6 and $\rho = 0.9$ have been performed. For the central settlement analyses for $\rho = 0.3$, $\rho = 0.6$, $\rho = 0.9$, $\rho = 1.2$, $\rho = 1.5$, $\rho = 1.8$ have been performed.

Figures 26-34 show the evolutionary history of the PI and the optimal topology. For each case the maximum value PI_{max} of the performance index as well as the corresponding value V_f of the volume fraction of the initial domain are indicated.

Figures 26-28 regard the case of the settlement that involves the lateral part of the wall while figures 29-34 refer to the case of the settlement that involves the central part of the wall.

Regarding the lateral settlement, in all cases under study (Figs. 26-28), BESO results show that loads located either above the settlement area or close to that area follow a path similar to $LP(5)$ in Figure 14.

A difference can be noted for the other loads. In fact, for ρ equal to 0.3 or 0.6 (Figs. 26 and 27) the other loads follow a direct compression path generating an additional compression longitudinal chord in the middle of the wall (i.e. $LP(3)$ of Fig. 12). According to the LPM, this is a direct consequence of the circumstance that, for ρ equal to 0.3 or 0.6, these loads, undergoing a slight deviation, generate thrusts very low in value. It follows that the strain energy of the middle longitudinal chord has to be very low too. This is the reason why, in this scenario, in order to save strain energy, the travelling loads prefer to follow the shortest path (i.e. the direct compression one).

On the other side, for $\rho = 0.9$ (Fig. 28), loads which are not close to the area involved by the settlement, undergo not negligible deviations and hence follow a path similar to $LP(5)$ in figure 14 in order to save strain energy (i.e. that associated to the middle longitudinal chord).

With respect to the central settlement, if it is very small (i.e. $\rho = 0.3$; Fig. 29), loads follow a direct compression path like that of $LP(3)$ in figure 17. For larger settlement (Figs. 30-34), loads either above or close to the area involved by the settlement follow a path similar to $LP(5)$ in figure 19, whereas the other loads follow a direct compression path like that of $LP(3)$ in figure 17. It has to be highlighted that, for very large settlement (i.e. $\rho = 1.8$; Fig. 34), most of the loads above the settlement seem to follow a path similar to that of $LP(2)$ (Fig. 16).

It is worth noting that for $\rho \geq 0.6$ (Figs. 30-34) and regarding loads either above or close to the area involved by the settlement, the descending path from the top to the bottom of the wall, sometimes tends to be diagonal like that of $LP(2)$ in figure 16. According to the LPM, this circumstance can be justified as the activation of the so-called 'arch-behaviour' ([22], [27], [28]).

From the comparison between these results and those presented in paragraph 4, it can be noted that, with respect to loads either above or close to the area of the settlement, the LPM approach essentially gives the same results as the BESO approach. This means that, as suggested by Mezzina et al. ([27], [28]), because of the time needed to perform BESO analyses, this evolutionary optimization procedure can be used as optional (e.g. for complex cases) in order to validate (e.g. only for limited parts of the structure under study) the results obtained by using the
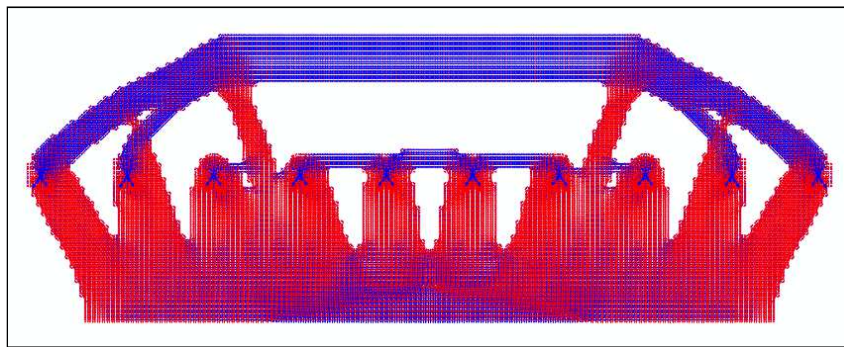
F. Palmisano, A. Elia

Load Path Method.

Fig. 26. Settlement that involves the lateral part of a masonry wall. BESO analysis. Optimal shape ($PI_{max} = 1.29$; $V_f = 61\%$; red = compression; blue = tension) in the case of $\omega = 1$ and $\rho = 0.3$

Fig. 27. Settlement that involves the lateral part of a masonry wall. BESO analysis. Optimal shape ($PI_{max}=1.30$; $V_f = 62\%$; red = compression; blue = tension) in the case of $\omega = 1$ and $\rho = 0.6$

Fig. 28. Settlement that involves the lateral part of a masonry wall. BESO analysis. Optimal shape ($PI_{max}=1.25$; $V_f = 77\%$; red = compression; blue = tension) in the case of $\omega = 1$ and $\rho = 0.9$
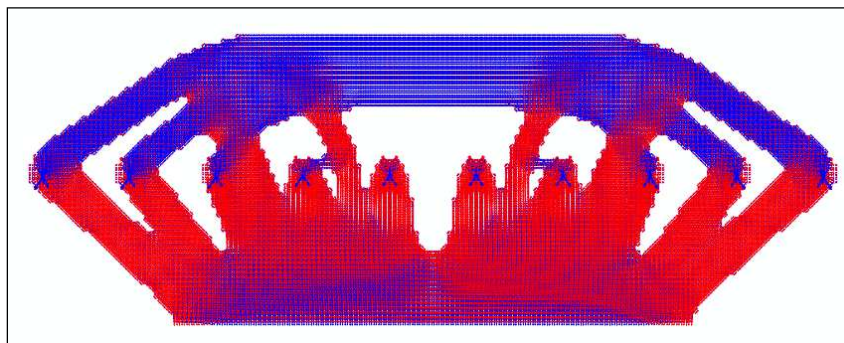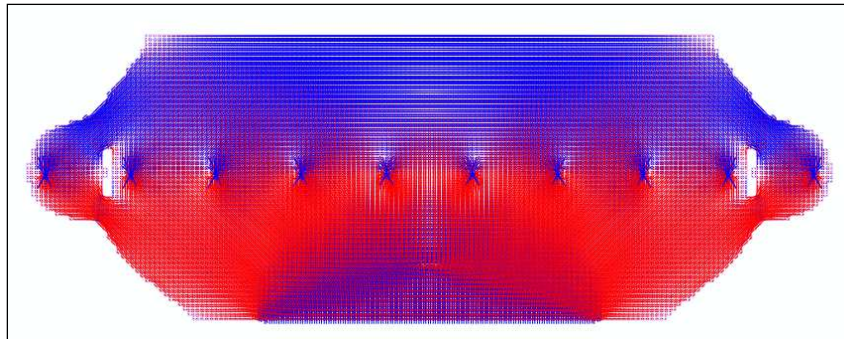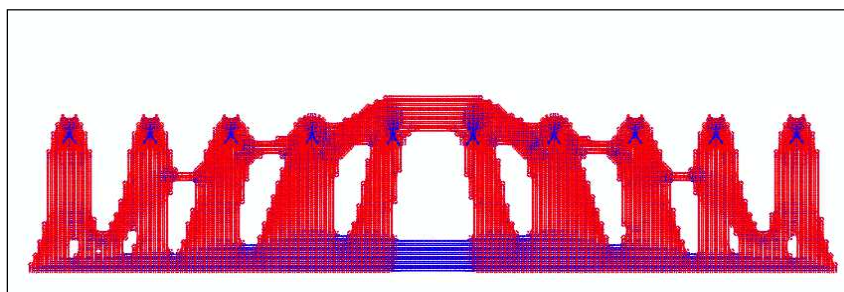

Fig. 29. Settlement that involves the central part of a masonry wall. BESO analysis. Optimal shape ($PI_{max}=1.58$; $V_f = 40\%$; red = compression; blue = tension) in the case of $\omega = 1$ and $\rho = 0.3$
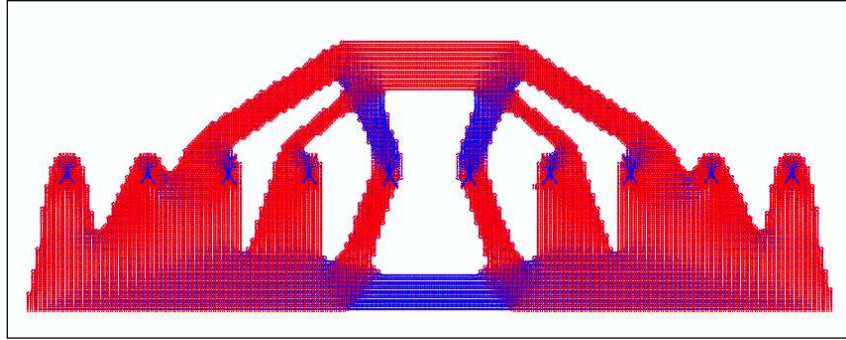
Fig. 30. Settlement that involves the central part of a masonry wall. BESO analysis. Optimal shape (PI_{max}=1.37; V_f = 55%; red = compression; blue = tension) in the case of ω = 1 and ρ = 0.6

Fig. 31. Settlement that involves the central part of a masonry wall. BESO analysis. Optimal shape (PI_{max}=1.14; V_f = 77%; red = compression; blue = tension) in the case of ω = 1 and ρ = 0.9

Fig. 32. Settlement that involves the central part of a masonry wall. BESO analysis. Optimal shape (PI_{max}=1.13; V_f = 86%; red = compression; blue = tension) in the case of ω = 1 and ρ = 1.2

Fig. 33. Settlement that involves the central part of a masonry wall. BESO analysis. Optimal shape (PI_{max}=1.14; V_f = 83%; red = compression; blue = tension) in the case of ω = 1 and ρ = 1.5
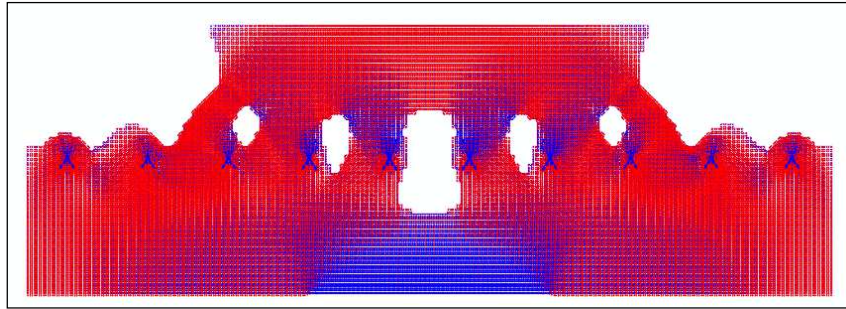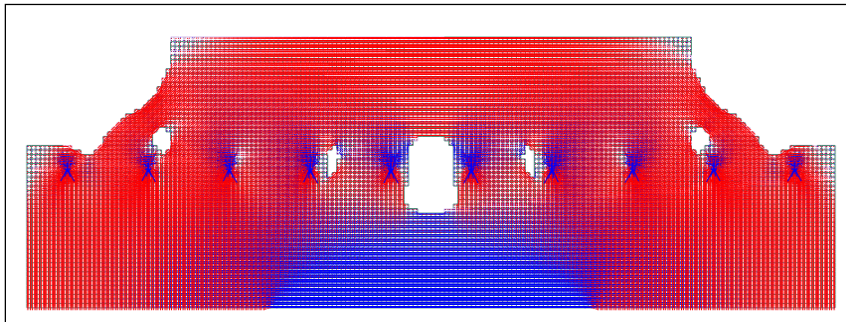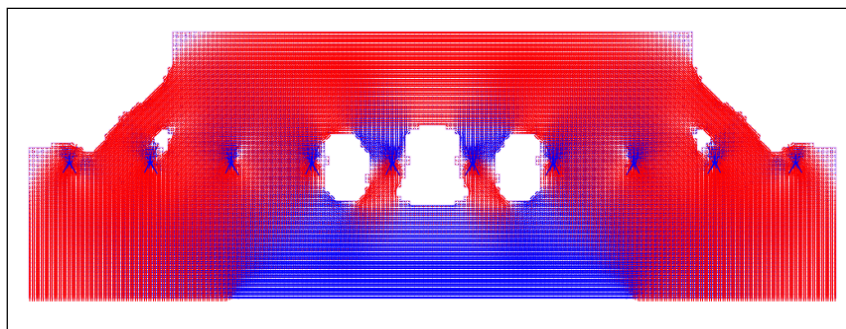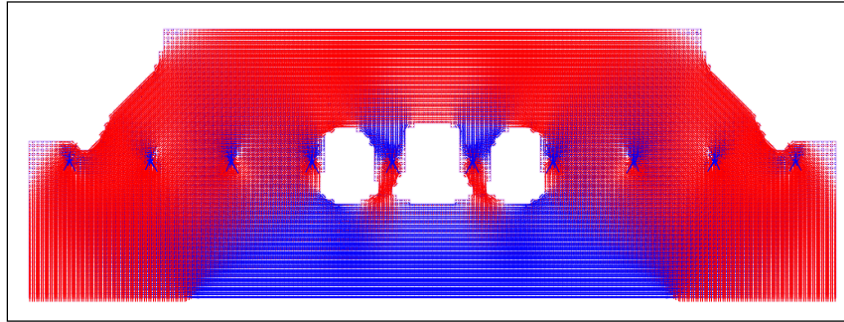
F. Palmisano, A. Elia

Fig. 34. Settlement that involves the central part of a masonry wall. BESO analysis. Optimal shape (PI_{max}=1.13; V_f = 83%; red = compression; blue = tension) in the case of $\omega = 1$ and $\rho = 1.8$

6. An Application of the Load Path Method to the Diagnosis of Crack Patterns

One of the main difficulties, when dealing with landslide structural vulnerability, is the possibility to individuate the causes of assessed cracks. Models based on classical structural mechanics are often difficult to apply especially when there is the necessity to perform a rapid vulnerability assessment at the territorial scale.

This paragraph aims to show that the Load Path Method, thanks to its versatility, can be also effective in the diagnosis of crack patterns of masonry structures due to landslide movements.

The proposed approach starts from the consideration that a structure, during its life, undergoes several 'evolutions'. The whole process can be brought back to the sequence of a limited number of instantaneous 'configurations' (i.e 'States'), each one caused by a specific 'State Transformation'. Structural behaviour analysis can be reduced to the verification of those configurations and of the relevant transformations [35].

If dealing with masonry structure the following states can be defined:

- *State 0*: the structure is not stressed.
- *State 1*: the structure is stressed but there are no cracks.
- *State 2*: first cracks appear.
- *State 2a*: cracks become larger and new cracks appear (i.e. crack evolution state).
- *State 3*: ultimate limit state. The structure is heavily damaged with no residual strength and stiffness (i.e. the structure is not capable of sustaining further loads).

In this paragraph an example of the application of the interpretation of crack patterns by using the LPM is showed.

Models in paragraph 4 have demonstrated that two main categories of tensile flux can be defined in a masonry wall subjected to a lateral settlement: diagonal and longitudinal. This means that two main crack patterns can be defined: one due to the diagonal tensile flux and the other due to the longitudinal tensile flux.

Obviously, it is also possible to find more than one crack pattern type in a masonry wall; it depends on the 'evolution' that the wall has undergone from *State* to *State*.

In figure 35 a model of the generation of an arch-shaped crack (Fig. 36) is shown.

According to models presented in paragraph 4, after the soil settlement (*State 1a*) part of the loads follow an inclined ascent path (Fig. 35a) in order to find a new equilibrated configuration. When the stress in an inclined path in tension reaches the tensile strength of the masonry wall (*State 2*), the first crack is generated (Fig. 35b). The consequent bypass of this crack generates a concentration of tensile stresses around the fissure (because loads, in order to minimise strain energy, tend to follow shorter paths) that causes the extension of the crack up to its stabilisation (end of *State 2a*; Fig. 35c). In such phase, the part of the masonry panel underneath the crack finds again the contact with the soil and, consequently, relevant loads restart to follow a path similar to that of *State 1*. On the other side, loads above the crack are now obliged to move out of the crack and then can cause further cracks at the top of the masonry wall.

It is worth noting that the exact shape of the final crack depends on geometry, load distribution and position of the first cracks. Sometimes the arch-shaped crack can degenerate into a diagonal crack (Fig. 37).
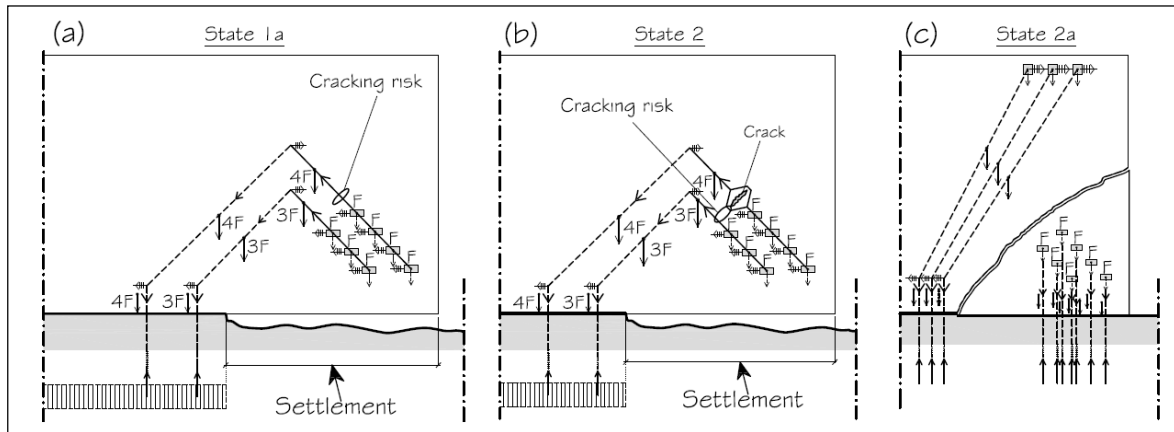
Fig. 35. Formation of a half arch-shaped crack due to lateral settlement

Fig. 36. Half arch-shaped crack on a building in Pietramontecorvino (Puglia, Italy)

Fig. 37. Diagonal crack on a building in Bovino (Puglia, Italy)

7. Conclusions

According to data presented in October 2011 at the Second World Landslide Forum (Rome, Italy), damages caused by landslides in the most industrialised country in the world are worth more than € 6 milliard annually. This is the reason why a methodology to reduce landslide risk is needed.

Following Roca et al. [8], who sustain simple methods

F. Palmisano, A. Elia

based on fundamental principles (e.g. limit theorems of plasticity) as still crucial to catch on the primary aspects of the structural response, this article has been devoted to demonstrate the effectiveness of the Load Path Method in the interpretation of the behaviour of masonry buildings subjected to foundation settlements due to landslide.

Models useful for understanding brick-mortar interface behaviour as well as the global one have been reported. The global proposed approach has been also validated by using Bi-directional Evolutionary Structural Optimization method.

One of the main difficulties, when dealing with landslide structural vulnerability, is the diagnosis of the causes of the crack pattern. This is also due to the excessive complexity of models based on classical structural mechanics, that makes them inappropriate especially when there is the necessity to perform a rapid vulnerability assessment at the territorial scale. This is the reason why a new approach, based on a simple model (i.e. the Load Path Method), has been here proposed for the diagnosis of crack patterns of masonry structures subjected to landslide movements. The effectiveness of the Load Path Method has been demonstrated for a case study.

In the article it has been shown that the load path method can be a versatile and effective instrument to study masonry structures because it seems to conciliate successfully the necessity to get a numerical solution without losing touch with the perception of the synthesis of physical structural behaviour.

Further theoretical work is needed in order to quantify the ultimate capacity of masonry walls in the above mentioned conditions. Nonlinear and anisotropic behaviour should be implemented in the method and comparison of the results with those of laboratory tests is needed.

Notations

A_i	transversal area of the ith side of a load path
$A_{sup,I}$	top transversal area of the ith strut
$A_{inf,i}$	bottom transversal area of the ith strut
b	semi-length of a wall
B	length of a wall
BESO	Bi-directional Evolutionary Structural Optimization
C_0	strain energy of the initial design under the applied loads
C_i	width of the bottom longitudinal chord or strain energy the current design at the i-th iteration in the BESO analysis
C_s	width of the top and of the bottom longitudinal chord
D	strain energy
D_i	elementary strain energy of the side i of a load path
D_{REF}	reference strain energy
E	end of a load path
E_c	compression Young's Modulus of the wall
E_c	tension Young's Modulus of the wall
F	travelling load
h	$H/2-\delta_s$
H	thrust of a travelling load or total height of a wall
i	generic side of a load path
l_i	length of the side i of a load path
n	mesh number of the semi-length b of the wall
N_i	intensity of the vector that bears the travelling load on the side i of a load path
LPM	Load Path Method
PI	Performance Index
S	start of a load path or thickness of a wall
STM	Strut-and-Tie Model
V	integration domain
W_i	actual weight of the domain at the i-th iteration
W_0	actual weight of the initial domain
x_a	mesh width of the wall in the X direction of the panel
x_b	mesh width the reactive soil in the X direction
α	length of the soil settlement
δ_s	position, along the Y direction, of the load deviation nodes at the top of the wall
ε	strain vector
ε_i	mean strain on the side i of a load path
ω	ratio of the compression Young's Modulus of the wall to the tension one
σ	stress vector
θ_I	inclination of the ith strut
γ	unit weight of the wall
ρ	ratio of the soil settlement to the height of the wall

References

[1] Cotecchia F, Vitone C, Cafaro F, Santaloia F. The mechanical behaviour of intensely fissured high plasticity clays from daunia. invited paper. characterisation and engineering properties of natural soils, Procceding of the Second International Workshop on Characterisation and Engineering Properties of Natural Soils, Singapore, KK Phoon, DW Hight, S Leroueil, TS Tan eds., Taylor & Francis, London, UK, 2007, pp. 1975-2003.

[2] Cotecchia F, Lollino P, Santaloia F, Vitone C, Mitaritonna G. A research project for deterministic landslide risk assessment in Southern Italy: methodological approach and preliminary results, Proc. of the 2nd International Symposium on Geotechnical Safety and Risk, Nagara, Japan, 2009, pp. 363-370.

[3] Vitone C, Cotecchia F, Desrues J, Viggiani G. An approach to the interpretation of the mechanical behaviour of intensely fissured clays, Soils & Foundation Journal, Japanese Geotechnical Soc, Tokyo, Japan, 2009, No. 3, Vol. 49, pp. 355-368.

[4] Cotecchia, Santaloia F, Lollino P, Vitone C, Mitaritonna G. Deterministic landslide hazard assessment at regional scale, GeoFlorida 2010: Advances in Analysis, Modeling and Design (Geotechnical Special Publication No. 199), DO Fratta, AJ Puppala, B. Muhunthan eds, ASCE, USA,

2010, pp. 3130-3139.

[5] Vitone C, Cotecchia F. The influence of intense fissuring on the mechanical behaviour of clays, Géotechnique, Ice Publ, London, UK, 2011, No. 12, Vol. 61, pp. 1003-1018.

[6] Vitone C, Cotecchia F, Viggiani G, Hall SA. Strain fields and mechanical response of a highly fissured bentonite clay, International Journal for Numerical and Analytical Methods in Geomechanics, Vol. 37, 2013, pp. 1510-34.

[7] Vitone C, Viggiani G, Cotecchia F, Hall SA. Localized deformation in intensely fissured clays studied by 2D digital image correlation, Acta Geotechnica, 2013, No. 3, Vol. 8, pp. 247-63.

[8] Roca P, Viviescas A, Lobato M, Díaz C, Serra I. Capacity of shear walls by simple equilibrium models. International Journal of Architectural Heritage, 2011, No. 5, Vols. 4-5, pp. 412-35.

[9] Lourenço PB. Computations of historical masonry structures, Progress in Structural Engineering and Materials, 2002, No. 3, Vol. 4, pp. 301–319.

[10] Ritter W. Die Bauweise Hennebique, Schweizerische Bauzeitung, 1899, No. 33, Vol. 7, pp. 59-61.

[11] Schlaich J, Schafer K, Jennewein M. Toward a consistent design of structural concrete, *PCI Journal*, 1987, No. 3, Vol. 32, pp. 74-150.

[12] Ganz HR, Thürlimann B. Strength of brick walls under normal force and shear, Procceding of 8th International Symposium on load bearing brickwork, London, UK, 1983, pp. 27–29.

[13] Roca P. Assessment of masonry shear walls by simple equilibrium models, Construction and Building Materials, 2006, No. 4, Vol. 20, pp. 229–238.

[14] Reineck KH, Lourenço MS, Almeida JF, Haugerud SA. Gaining experience with strut-and-tie models for the design of concrete structures, Design examples for strut-and-tie models, Fib Bulletin 61, 2011, pp. 197-216.

[15] Palmisano F, Vitone A, Vitone C. Form & structure, the rome auditorium: load path method (LPM), D'Architettura, 2002, Vol. 18, pp. 168-173.

[16] Palmisano F, Vitone A, Vitone C. From load path method to classical models of structural analysis, System-based Vision for Strategic and Creative Design, F. Bontempi ed, Balkema, Rotterdam, The Netherlands,. 2003, Vol. 1, pp. 589-596.

[17] Palmisano F. Form and structure in the harmonious complexity of the building process: from conceptual design to detailing in some reinforced concrete works, Structural Concrete, 2005, No. 3, Vol. 6, pp. 122-130.

[18] Palmisano F, Vitone A, Vitone C, Vitone V. Collapse of the Giotto Avenue Building in Foggia, Structural Engineering International, IABSE, Zurich, Switzerland, 2007, No. 2, Vol. 17, pp. 166-171.

[19] Palmisano F, Vitone A, Vitone C. A first approach to optimum design of cable supported bridges using load path method, Structural Engineering International, 2008, No. 2, Vol. 18, pp. 412-420.

[20] Vitone C. Il Load Path Method per il restauro strutturale delle opere murarie, M.S. thesis, Politecnico di Bari, Bari, Italy, 2001.

[21] De Tommasi G, Monaco P, Vitone C. A first approach to load path method on the masonry structures behaviour, Structural Studies, Repairs and Maintenance of Heritage Architecture VIII, CA. Brebbia ed, WITpress, Southampton, UK, 2003, pp. 287-296.

[22] Palmisano F, Vitone A, Vitone C. Load path method in the interpretation of the masonry vault behaviour, Structural Studies, Repairs and Maintenance of Heritage Architecture IX (Advances in Architecture Series 20),

CA Brebbia & A. Torpiano eds, WITpress, Southampton, UK, 2005, 155-167.

[23] Palmisano F, Totaro. Load path method in the interpretation of dome behaviour, Structures & Architecture, Proccedign of the 1st International Conference on Structures & Architecture, Guimarães, Portugal, 2010, Edited by PJS Cruz, CRC Press/Balkema, Leiden, The Netherlands, pp. 1826-1833.

[24] Palmisano F. Interpretation of the behaviour of masonry arches and domes by simple models, Structural Studies, Repairs and Maintenance of Heritage Architecture XIII (WIT Transactions on the Built Environment 131), edited by CA Brebbia, WITpress, Southampton, UK, 2013, pp. 233-244.

[25] Palmisano F. Assessment of masonry arches and domes by simple models, International Journal of Structural Engineering (IJSTRUCTE), 2014, No. 1, Vol. 5. pp. 63-75.

[26] Palmisano F, Elia A. Masonry buildings subjected to foundation settlements due to landslide: a preliminary study on the interpretation of structural behaviour using load path method, Structural Studies, Repairs and Maintenance of Heritage Architecture XI (WIT Transactions on the Built Environment 109), edited by CA Brebbia, WITpress, Southampton, United Kingdom, 2009, pp. 141-150.

[27] Mezzina M, Palmisano F, Raffaele D. The design of R.C. bridge deck subjected to horizontal actions by strut-and-tie model, Bridge Maintenance, Safety, Management and Life-Cycle Optimization, proccedign of the 5th International Conference on Bridge Maintenance, Safety and Management–IABMAS 2010, Philadelphia, Pensylvania, USA, July 11-15 2010), edited by D.M. Frangopol, R. Sause, CS Jusko, Taylor & Francis Group, London, UK, 2010, pp. 2390-2397.

[28] Mezzina M, Palmisano F, Raffaele D. Designing simply supported R.C. bridge decks subjected to in-plane actions: Strut-and-Tie Model approach, Journal of Earthquake Engineering, Taylor & Francis, London, UK, 2012, Vol. 16, No. 04, pp. 496-514.

[29] Xie YM, Steven GP. A simple evolutionary procedure for structural optimization, Computers & Structures, 1993, Vol. 49, pp. 885–886.

[30] Yang XY, Xie YM, Steven GP, Querin OM. Bidirectional evolutionary method for stiffness optimization, AIAA Journal, 1999, No. 11, Vol. 37, pp. 1483–1488.

[31] Huang X, Xie YM. Convergent and mesh-independent solutions for the bi-directional evolutionary structural optimization method, Finite Elements in Analysis and Design, 2007, Vol. 43, pp. 1039-1049.

[32] Abaqus 2007. User's Manual, Version 6.7.

[33] MIT (Ministero delle Infrastrutture e dei Trasporti) 2009. Circolare del Ministero delle Infrastrutture e dei Trasporti 2 febbraio 2009, No. 617. Istruzioni per l'applicazione delle "Nuove Norme tecniche per le Costruzioni" di cui al Decreto Ministeriale 14 gennaio, 2008.

[34] CEN (European Committee for Standardization). EN 1996-1-1:2005 Eurocode 6-Design of masonry structures-Part 1-1: General rules for reinforced and unreinforced masonry structures, 2005.

[35] Vitone A, Palmisano F, Vitone C. Load path method (LPM) in detailing design, Proccedign of 2nd International fib Congress, Naples, Italy (CD), 2006.

330

F. Palmisano, A. Elia